Effect of Phyllosilicates Rresence on Binder Hydration Characteristics and Hardening Process in Cemented Paste Backfills

Ikram Elkhoumsi[1], Tikou Belem[1], Mostafa Benzaazoua[1,2]

[1]Université du Québec en Abitibi-Témiscamingue, PQ, Canada, Ikram.Elkhoumsi@uqat.ca, tikou.belem@uqat.ca, mostafa.benzaazoua@uqat.ca
[2]Mohammed VI Polytechnique University (UM6P), Morocco, Mostafa.BENZAAZOUA@um6p.ma

Abstract
The decline in strength of cemented paste backfill (CPB) presents a recurrent challenge in underground backfilling operations. The heightened presence of phyllosilicates in CPB is recognized as a key factor contributing to its strength degradation. While some studies in civil engineering have delved into similar phenomenon, noting a decrease in concrete strength with rising mica content, there is conspicuous gap in research addressing this specific phenomenon within CPB.

This study systematically investigates the mechanical and hydrogeochemical responses of CPB influenced by phyllosilicates, specifically muscovite, addressing both quantitative and qualitative dimensions. The primary objective is to scrutinize the influence of varying muscovite contents on the hydration characteristics of the binding agent within CPB. The experimental program is meticulously designed to unveil significant changes in CPB physicochemical and mechanical properties across diverse muscovite contents (0%, 3%, 12% and 18%) throughout varying curing times (7 , 28, and 91 days). This investigation employs one binder type, general use Portland cement (Type GU) at two binder contents (Bw, 5 and 7%).

The findings from this study provide fresh perspectives on how phyllosilicates, particularly muscovite, impact the mechanical and physicochemical properties of CPB during both mixing and hardening phases. These insights contribute valuable knowledge for refining new CPB formulations (mix recipes) by thoughtfully considering the phyllosilicates content in mine tailings.

Key words: mine tailings, phyllosilicates, muscovite, cemented paste backfill, binding agent, formulation, curing time, hydration process, mix recipes, hardening, mechanical properties, physicochemical properties

Introduction
Phyllosilicate corresponds to a type of silicates minerals with a distinct crystal structure. It forms a large group of minerals including, among others, micas, chlorite, serpentinite, and kaolinites. Their basic characteristic is their layered structure responsible for their properties. Phyllosilicate minerals constitute ~ 40% of the mineralogical composition of mine tailings within the Abitibian district in Quebec, Canada (Ouffa, 2019). Consequently, they are present in large quantities in cemented past backfill as tailings constitute the main component in CPB mixtures.

Some studies in civil engineering have recognized the heightened presence of phyllosilicates in cementitious aggregates as a key factor contributing to its strength degradation (Dewar, 1963; Muller, 1971; Schmitt, 1990; Tarefder et al., 2014; Ko, 2019; Patil, 2021; Leemann et al., 2023). These studies have stated the negative influence of phyllosilicate, mainly mica group, on the mechanical behavior of concrete including the decline of comprehensive strength (Mshali & Visser, 2012; Tarefder et al., 2014; Tugrul et al., 2015; Leemann et al., 2023), the decrease of workability (Lagerblad et al., 2014) and the increase of water demand (Mshali and Visser, 2014; Maregesi et Salaam, 2020). In some of these studies, it was found experimentally that the inclusion of mica in fine aggregates contributes to a decline in compressive strength of concrete down to 8–23% range and an increase in water demand of concrete up to 16% (Maregesi and Salaam, 2020). Furthermore, it was reported that engineering properties mainly

plasticity index and compatibility of cemented aggregates are negatively influenced by the incorporation of high amount of mica (Mshali and Visser, 2014). The findings of this study have demonstrated a decrease of compacted density, difficulty in achieving high compaction with high mica content and an increase in water absorption from 3% to > 10% by mass for 10% of mica content (Mshali and Visser, 2014). A similar study (Prince, 2001) has reported that the presence of only 1% of mica in concrete decreases the mechanical strength to approx 5%. Another study on mortar (Xing et al., 2014) has stated that compressive strength decreases significantly with increasing mica content at 28 and 60 days showing anomalies in the microstructure hardened cement past. In the light of these results, phyllosilicates could be considered as strength reducing minerals for CPB, especially muscovite, which has been investigated in most cited studies above. However, a similar phenomenon has not been explored within CPB nor understood in civil engineering, leading to a conspicuous gap in research addressing this phenomenon.

In this context, the following study aims to delve the mechanical and hydrogeochemical behavior of CPB in presence of phyllosilicate, mainly muscovite, that constitutes a very frequent mineral within Abitibian mine tailings used in the fabrication of CPB. As a first target, an investigation of the influence of muscovite on the mechanical, physicochemical, and microstructural properties of CPB is conducted. For this purpose, a systematic approach, addressing both quantitative and qualitative dimensions is adopted. First, mixtures of CPB were prepared by using one fixed solid content (75%) and four diverse muscovite content (0, 3, 12, and 18%) throughout varying curing times (7, 28, and 91 days). Only one binder employed Type GU at two binder contents (5% and 7%). Second, additional CPB mixtures at constant slump were made to evaluate the water demand required in function of muscovite content. In both steps, mine tailings were substituted with pure silica to delve the mechanical properties exclusively related to the binder used without any further interactions from other ingredients.

The findings from this study provide fresh perspectives on how muscovite impact the mechanical and physicochemical properties of CPB during both mixing and hardening phases, offering valuable insights for refining new CPB formulations (mix recipes) by thoughtfully considering the phyllosilicates content in mine tailings.

Materials

Sil-Co-Sil 106

Pure silica, in the form of SIL-Co-SIL, was used to simulate mine tailings in the preparation of CPBs to avoid the complexity of possible interactions between different mineralogical compounds of mine tailings (Ercikdi et al., 2009; Benzaazoua et al., 2004). SIL-Co-SIL® 106 (US Silica, USA) was chosen because of its consistent chemistry and its particle size distribution (PSD) corresponding to the average of PSD for 9 mines tailings in the Abitibi sector (Sadatalhosseini et al., 2014).

Muscovite

Muscovite employed in this study was sampled from a pegmatitic deposit mineralized in columbite-tantalite within the Aldous mineralized zone, located in the Abitibi province. Raw muscovite was passed though numerous preparation steps including sorting, drying, crushing, and sieving processes to obtain a clean and refined muscovite powder. Muscovite (Msc) was pulverized at speed of 300 tr/min using a planetary ball mill, to obtain a powder with a particle size of P20 µm corresponding to the average of P20 µm for four mines tailings in Abitibi sector (P20 = 35.3 µm). This condition confirms the homogeneity of prepared muscovite within the fine fraction of tailings (d < 20µm). It was assumed, based on internal work, that muscovite accumulates in the finer fractions of mine tailings (d < 20 µm). This assumption complies with some studies conducted on crushed rocks aggregates that experimentally approved that free mica accumulates in fine fraction within a d < 24 µm (Loorents, 2007) and/or d < 38 µm (Lagerblad, 2005), respectively.

Cement and Mixing Water

During this study, one binder used for the fabrication of CPB mixtures. The binder employed was Type GU, also referred to as ordinary Portland cement (OPC), which is widely used in backfilling operations (Tariq et al., 2014). As the chemistry of mixing water affects CPB behavior (Benzaazoua et al., 2002), it was suggested to use tap water (TW) in CPB production with the chosen binder. Tap water was collected to maintain the same water chemistry and quality through this study.

Methodology

Material characterization

Prior to CPB preparation, their ingredients were characterized physically and chemically. Specific gravity (G_s) of muscovite, pure silica and Type GU cement were measured respectively, using an automatic gas pycnometer (ULtrapyc 1200e, Quantachrome Instruments). Specific surface area (S_s) of materials was analyzed through the BET method (Braunauer-Emmett-Teller) using nitrogen liquid (Gemini 2375, Micromeritics). Particle size distribution (PSD) was analyzed by a laser diffraction particle size analyzer (Malvern Mastersizer 3000). The chemical composition was obtained by X-ray fluorescence spectrometry (S2 Ranger, Bruker AXS). Inductively Coupled Plasma Mass Spectrometry (ICP-MS), Agilent 7800) was used for the chemical analysis of mixing water. pH and conductivity of tap water was also analyzed using a multimeter (B30PCI, VWR SympHony).

CPB Preparation, Moulding and Curing

The first set of CPB mixtures were prepared considering a constant solid content (75%). Cement contents for all CPB mixtures were chosen as either 5 wt% or 7 wt%. To explore the influence of muscovite content, four diverse muscovite contents (0% control mixture, 3%, 12%, 18%) were used in the preparation for CPB mixtures. CPB design recipes including the selection of binder and muscovite contents were determined by the experimental plan of Taguchi (Pillet, 2001). The required masses of each ingredient were calculated using an Excel spreadsheeted developed by Belem et al. (2016), based on the following equations:

Solid content (%),

$$C_w = \frac{M_s}{M_{tot}} = \frac{M_T + M_{sc} + M_B}{M_s + M_w} \quad \text{Equation 1}$$

Binder content,

$$B_w = \frac{M_B}{M_T + M_{Msc}} \quad \text{Equation 2}$$

Muscovite content,

$$Msc = \frac{M_{Msc}}{M_T + M_{Msc}} \quad \text{Equation 3}$$

Ratio,

$$R = \frac{M_w}{M_B + M_{Msc}} \quad \text{Equation 4}$$

These equations represent, respectively, the mass of tailings, muscovite, and binder within the total mass of CPB . The mass of water in the paste, *R*, is a defined as a ratio between water, cement, and muscovite to include the effect of muscovite in the mix design. The distribution of ingredients within CPB in presence of muscovite is presented in Figure 1.

Table 1 presents the formulations and characteristics of each recipe prepared respectively with 5% and 7% of binder, 0% to 18% of muscovite, hereafter referred to as X%-CPB-Y%-Z, where X and Y correspond to binder content , muscovite content , and Z curing time in days, respectively. Ingredients were blended

using a Hobart mixer. Mixing duration was set to 7 min. Once blended, a proportion of the CPB was used to measure the backfill slump then returned to the mixer to ensure homogenisation. Once prepared, the pastes were poured into cylinder-shaped molds (D*H:51*100 mm) in a single layer, tapped 25 times and shaken sideways to expel air bubbles from the backfill past. Prepared molds are hermetically sealed and kept in a controlled atmosphere chamber with a relative humidity of around 90% and a temperature of 25ºC ±2ºC. Each recipe was produced in triplicates for each curing time (7, 28, and 91 days) to ensure the reliability of experimental results and reduce bias.

The second set of CPB mixtures was prepared in an identical manner, except for the addition of water to achieve a target slump. More details about the preparation are available in a later secion (Water Demand Tests).

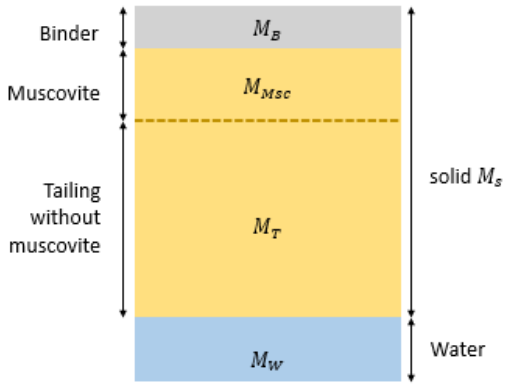

Figure 1. Schematic representation of CPB with muscovite (ingredients distribution is approximative).

Table 1. Formulations and characteristics of simulated CPB recipes.

Mixture					
5-CPB-0%	75%	GU	7	7	7d, 21d, 91d
5-CPB-3%	75%	GU	7	4.38	7d, 21d, 91d
5-CPB-12%	75%	GU	7	2.06	7d, 21d, 91d
5-CPB-18%	75%	GU	7	1.52	7d, 21d, 91d
7-CPB-0%	75%	GU	5.1	5.1	7d, 21d, 91d
7-CPB-3%	75%	GU	5.1	3.57	7d, 21d, 91d
7-CPB-12%	75%	GU	5.1	1.88	7d, 21d, 91d
7-CPB-18%	75%	GU	5.1	1.43	7d, 21d, 91d

Slump-cone tests

For the process of evaluating the effect of muscovite on the consistency of prepared CPB mixtures, the slump-cone test was adopted (Belem et al., 2003). Slump measurements of all mixtures were determined by using a miniature slump cone in conformity with ASTM C143. The mini-cone used in other studies proved effective (Roussel et al., 2005; Tan et al., 2017). It consists of a truncated cone with half the dimensions of the standard Abrams cone (ASTM C143; bottom diameter 100 mm, top diameter 50 mm, height 150 mm). The test procedure follows that described for the standard slump test (Figure 2). The mini

cone was selected due to the lower amount of material available for laboratory testing. A conversion factor of 2.28 () was considered for converting the mini slump measured for CPB mixtures to the corresponding standard Abrams cone slump based on available in-house laboratory investigations and literature data (Outtara, 2017).

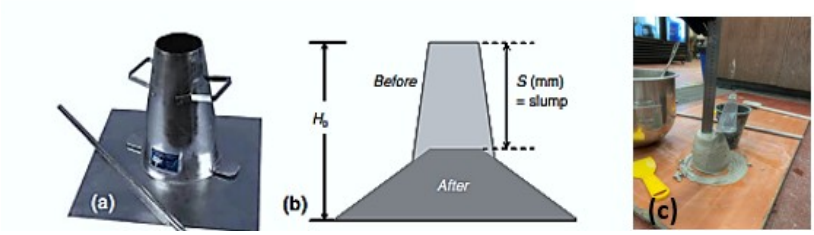

Figure 1. Slump measurement with mini cone: a) illustration of mini cone used; b) schematic illustration of the slump test procedure (Belem et Benzaazoua, 2008; de Ferraris et de Larrard, 1998); c) home-lab measurement of slump for CPB design at C_w = 75% and muscovite content = 18%; measured slump was found in the order of 6.1 cm.

Unconfined Compression tests

After curing (7, 28, and 91 days), CPB mixtures were subjected to unconfined compression tests carried out using MTS 10/GL mechanical press with an axial loading capacity of 50kN and minimum strain rate of 1,mm/min. UCS test were conducted in conformity to ASTM C39. All the measurements were carried out in triplicate and the average values were taken as the final compressive strengths. The effect of muscovite content on the UCS of CPB mixtures was also estimated, and represent mechanical strength of mixtures with muscovite and mixture of control (without muscovite):

$$\frac{UCS_1 - UCS_0}{UCS_0} \qquad \text{Equation 5}$$

After UCS measurements, a subsample of each specimen was selected, weighed, and oven-dried (60◦C) to assess the water content of the samples after curing. Other collected specimens were dryied through a systematic approach to stop hydration, then kept for further complementary analyses, including, X-ray diffraction (XRD), Fourier transform infrared spectroscopy (FTIR), and DRX. Hydration stoppage consisted of replacing free water within CPB with isopropanol, which is further eliminated through evaporation; more details about this approach can be found in Snellings et al., 2018.

Microstructural Analysis

To examine the hydration products of the studied CPB mixtures, XRD and FTIR analyses were used. FTIR is a qualitative analysis that enables the chemical nature of a sample to be reconstructed by identifying the absorption bonds in a spectrum. The technique was used to identify and compare the chemical bands formed in the presence of muscovite. Adopted protocol consists of introducing 15% by mass of sample into KBr, then grinding the whole sample before analysis. Spectral analysis was carried out in the 4000–500 cm^{-1} range, with a spectral resolution of 4 cm^{1}, in DRIFT mode, and recorded in absorbance mode. Spectra are corrected for baseline to improve analysis accuracy. XRD analysis was carried out to determine semi-quantitatively the mineral composition and content of fill hydration products. For both analyses, only 7-CPB-Y% mixtures at 7 days were examined.

Physicochemical Properties

Samples from each CPB mixture were analyzed for various characterization tests (water content, specific surface area, chemical composition) to explore changes on CPB properties under the effect of muscovite. Table 2 summarizes the selected CPB mixtures studied for each analysis.

Table 1. Selected CPB mixture by testing method.

Testing method	SS	XRD	FTIR	XRF
Analyzed mixtures	5%-CPB-%Msc-7j 7%-CPB-%Msc-7j 7%-CPB-%Msc-28j	7%-CPB-%Msc-7j 7%-CPB-%Msc-28j	7%-CPB-0%-91j 7%-CPB-3%-91j 7%-CPB-18%-91j	7%-CPB-%Msc-7j 7%-CPB-%Msc-28j 7%-CPB-%Msc-91j

%Msc indicates all muscovite contents (0, 3, 12, and 18%)

Water Demand Tests

The effect of different muscovite contents on water demand was evaluated by producing the same CPB recipes and varying the mass of water added to the mixture. Mixing water was added to the pastefill step by step until reaching the target past consistency (slump), which corresponds to min-slump value of 8.5 cm ±0.5 cm. Control mixtures with 0% muscovite were first prepared to determine the reference water mass, which provides the target slump. Increased water demand ratio was calculated as following:

$$WD\% = \frac{M_{w1} - M_{w0}}{M_{w0}} \qquad \text{Equation 6}$$

where M_{w1} is the mass of water added to the mixture to achieve the target slump.

Samples from the prepared CPB were also poured, molded, and cured for further UCS measurements and water content analysis.

Results

Initial characterization of materials

Samples from each component were taken for various characterization tests. Table 2 summarizes physical characteristics of studied materials. Specific gravity was measured for each material used in the preparation of CPB mixtures as it is required for the calculation of CPB formulations. Gs measured values were found to be 3.29, 2.8 and 3.17 for muscovite, Sil-Co-Sil, and GU-cement, respectively. Figure 3 depicts the cumulative PSD curves of CPB ingredients to compare muscovite PSD with Sil-Co-Sil and ensure it has been properly pulverised. Table 2 also presents some of the main PSD indicators for characterizing the granulometric distribution of studied materials. The fine contents of these materials (P20 µm) are in the range of 35–52%. Curvature (C_c) and uniformity (C_u) coefficients indicate, respectively, well graded materials with different size ranges especially for muscovite (Cu = 19). Specific surface area (SS) values were found between 0.14 g for pure silica and 2.48 g for muscovite.

The chemistry of materials was also analyzed (Figure 4). SiO2 and Al2O3 are the dominant compounds for all the materials with contents values found to be 46.9–37.59% for muscovite, 97.22–2.5% for Sil-Co-Sil, and 23.36–7.12% for GU. For GU cement, the CaO is the dominant compound with 61.86%. Tap water chemistry results are presented in Table 3.

Table 2. Major experimental parameters of materials used in CPB design..

Parameter	unit	Muscovite	Sil-Co-Sil ®	GU-cement
Specific gravity, Gs,	(-)	3.29	2.8	3.17
Specific surface, SS,	/g	2.48	0.14	2.17
	µm	2.90	2.3	4.42
	µm	15.3	10.2	11.1
	µm	55.3	32.7	23.8
=	(-)	19.07	14.22	5.38
=*)	(-)	1.46	1.38	1.17
	%	34	44	50
	%	78	90	98

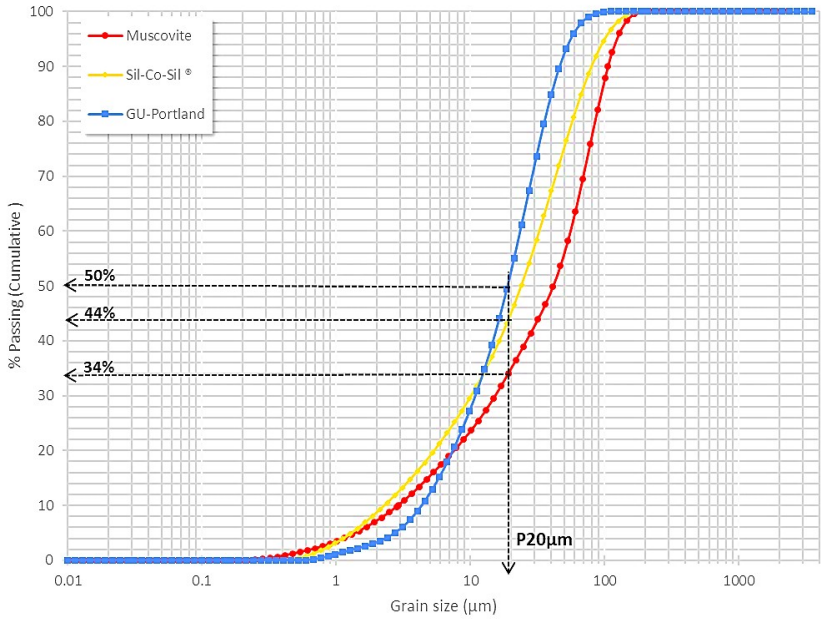

Figure 3. Cumulative particle size distribution of materials.

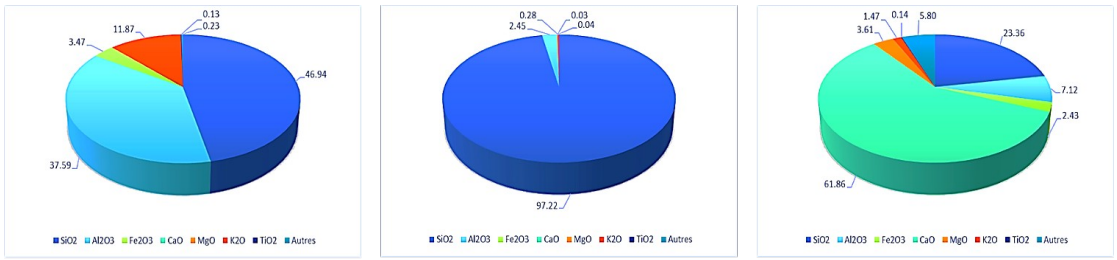

Figure 4. Chemical composition of studied materials.

Table 3. Chemistry of mixing water

Parameter	pH	EC	Eh	Ca	K	Cl	Mg	Si	Al	Cu	Fe	Na	S
Unit	-	µS/cm	V	mg/									
Tap water	7.6	0.0009	0.4	0.18	0.27	n/a	0.09	n/a	0.04	0.01	0.00	0.58	n/a

Influence of muscovite contents on mechanical strength

Figure 5 displays changes in the mechanical strength of CPB mixtures with different contents of muscovite (0, 3, 12, and 18%) and exposed to diverse curing times (7, 28, and 91 days).

The strength of CPB mixtures decreases as the muscovite content increases at all curing times (Figure 5a b). All the mixtures present a continuous increase of UCS with curing time. However, a noticeable drop of strength, at all tested curing times, is observed when muscovite content increases. The reductions in strength for all CPB mix varied proportionally depending on muscovite content. An increase in muscovite content by 3% reduces strength at 7 days from 718.6 kPa to 568.2 kPa and from 854 kPa to 689.3 kPa for 5%-CPB and 7%-CPB mixtures, respectively (Figure 5 (c)). This represents a strength failure rate (FR) of 20.9% and 19.3%, respectively. The FR results (Figure 5d) shows that the higher the muscovite content is in the mixture, the higher the strength rate failure. For instance, increasing the muscovite content within 5% and 7% mixtures from 0% to 18% contribute to a drop in UCS-7d in order of 36.8% and 29.4 %, respectively. The failure rate increases generally with curing time for high muscovite contents (12%, 18%) except for mixtures with 3% muscovite content, where the FR tends to decrease with curing time indicating a possible strength redemption over time at low muscovite content. However, this is not possible when muscovite content is high. It is also noted that the FR at 28 days for both binder contents at 12% and 18% muscovite content is lower than the FR at 7 days or 91 days (Table 4). This can be explained by a high rate of hydration, comparing to other mixtures, responsible for strength gain at 28 days minimizing the failure rate. Taking to account that w/r is constant for all mixtures (7 for 5% binder and 5.10 for 7% binder), it is more probable that CPB-mixture properties (eg, specific surface area, SS) are responsible for accelerating the hydration rate . The higher the SS, the larger the surface available for hydration, and consequently the higher the chance of a potential strength gain.

The decreases in mechanical strength tend to slow down after a certain muscovite enrichment (12%) as it shown in Figure 5c. For example, the 7d-UCS at 7% binder decreases from 854 kPa with 0% muscovite content to 689.3 kPa with 3% muscovite content, corresponding to a strength failure rate of about 19.3%, and from 608.3 kPa at 12% Msc to 602.6 kPa at 18% Msc, corresponding to a strength failure of 0.7% for 6% muscovite enrichment. This trend is also observed for mixtures with 5% cement and at all curing times (28 and 91 days). This tendancy can be interpretated in the context of void filling, where small muscovite quantities fill in available spaces between gravel particles (Mshalli et Visser, 2012). Another interpretation could be related to the lower amount of water available in the mixture comparing to the high muscovite content. These observations prove the phenomenon of strength decrease in CPB with rising mica content as it has delved in concrete in civil engineering. In addition, it seems that the understanding of the effect of muscovite on cement hydration and thus UCS development is highly related to the microstructural interactions between muscovite and binder, and muscovite and water.

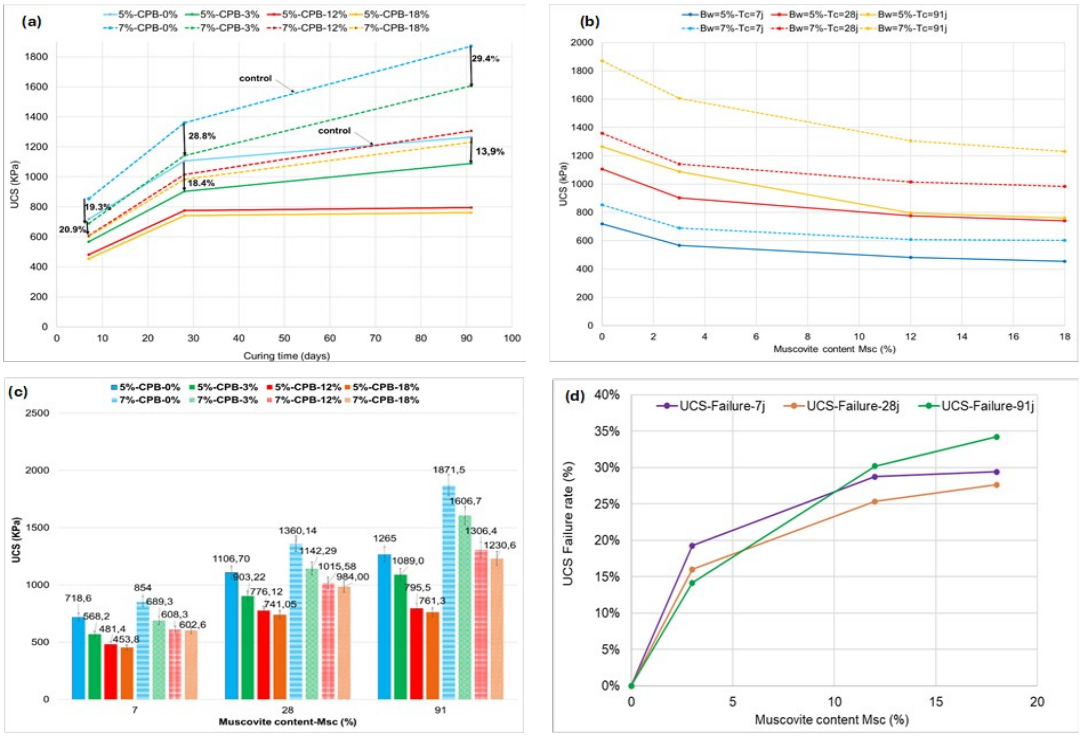

Figure 5. (a) UCS-curing time plots of CPB-mixtures with different muscovite contents: (a) Bw=5% and 7%; (b) & (c) UCS-muscovite content plots for 5% and 7% binder; (d) UCS failure rate-muscovite content plot for all curing times (7, 28, and 91 days).

Table 4. UCS Failure rate values for prepared mixtures.

Mix	FR-7j	FR-28j	FR-91j
5%-CPB-0%	0.0%	0.0%	0.0%
5%-CPB-3%	20.9%	18.4%	13.9%
5%-CPB-12%	33.0%	29.9%	37.1%
5%-CPB-18%	36.8%	33.0%	39.8%
7%-CPB-0%	0.0%	0.0%	0.0%
7%-CPB-3%	19.3%	16.0%	14.1%
7%-CPB-12%	28.8%	25.3%	30.2%
7%-CPB-18%	29.4%	27.7%	34.2%

Effect on CPB consistency

Figure 6 presents slump results in function of muscovite contents. Results show that the addition of muscovite resulted in a decreased in the slump of the mixtures. Increasing muscovite content from 0 to 18% led to a decrease in the slump from 8.2 to 6.1 cm for mixtures with 5% GU and from 8.3 to 6.4 cm for mixtures with 7% GU. Table 5 presents the standard Abrams slump values using a conversion value of 2.28. The slump is an index on the workability of CPB mixtures, which indicates a negative effect of muscovite content on the workability of the CPB. The higher muscovite content, the lower its consistency.

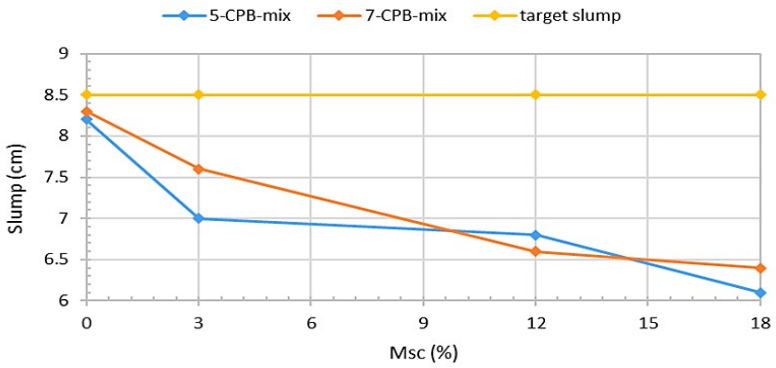

Figure 6. Effect of muscovite on the variation of slump results

Table 5. Results of the slump of the CPB mixtures

Mixture	mini-S (cm)	Abrams-S (cm)
5-CPB-0%	8.2	18.69
5-CPB-3%	7.0	15.96
5-CPB-12%	6.8	15.50
5-CPB-18%	6.1	13.90
7-CPB-0%	8.3	18.92
7-CPB-3%	7.6	17.32
7-CPB-12%	6.6	15.04
7-CPB-18%	6.4	14.59

Effect on microstructural and physicochemical properties of CPB

Specific surface area (S_S)

Figure 7 displays the variation of SS in function of muscovite content. Results show a general decrease in SS with increased muscovite content. Curing time seems to have a pronounced effect on the evolution of specific surface as at 28 days, the SS of 7% CPB mixtures ranges between 1.44–0.47 m^2/g for 0% and 18 % of muscovite content. However, at 7 days 7% CPB and 5% CPB mixtures only vary between 0.15m^- 0.05 m^2/g, and 1.08–0.95 m^2/g, respectively for the same content of muscovite. Consequently, it is shown that the higher the muscovite content, the lower the SS, hence the lower the surface available for hydration which helps to explain the strength loss. Variations in SS could also be explained by variations in the pore size distribution (Mehdipour et al., 2017), the E/C ratio (Seifi et al., 2023) or early hydration (Mantellato et al., 2015). A higher SS leads to greater reactivity and a denser microstructure, which can lead to higher strength and inversely. This can result because of a poor compaction and/or incomplete hydration process that restrain the development of the microstructure of CPB. These findings align with compaction problems cited in Mshalli et Visser, 2012 because of the high amounts of mica contents. However, complementary analysis is required to characterize and investigate hydration process in presence of muscovite.

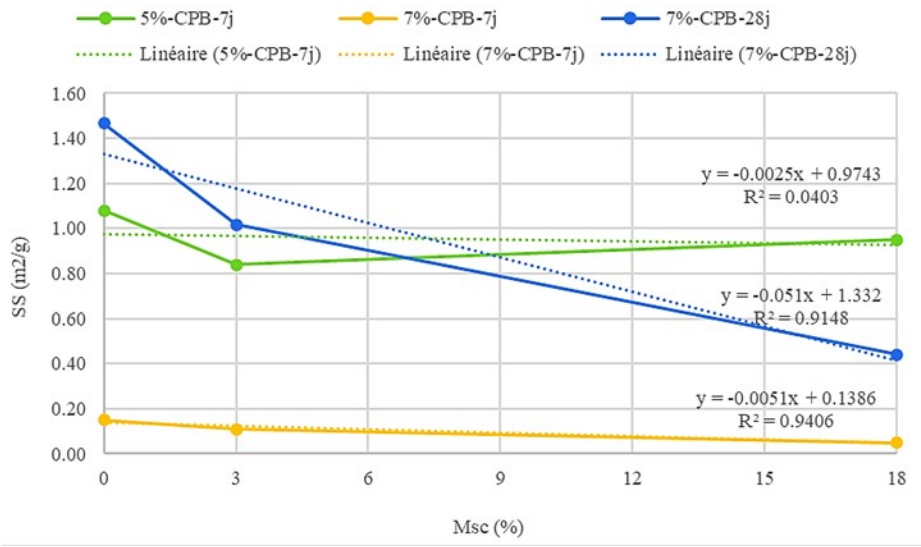

Figure 7. Specific surface variation in function of muscovite for some CPB-mixtures.

Mineralogy by XRD

Table 7 displays XRD results of 7 and 28 day cured mixtures with diverse muscovite contents (0, 3, 12, and 18%) and prepared with 7% GU binder. Results show that mineralogical composition of all mixtures is quartz-dominated due to pure silica within CPB mixtures. Muscovite is the second dominated mineral in the mixtures. However, muscovite semi-quantitative results seem to be quantitatively underrated for all mixtures. For instance, a 7% CPB/18% muscovite content is estimated to equal 6.4 and 4.9 at 7 and 28 days, respectively. Fill hydration products are found to be the same for all mixtures of calcite and portlandite at differing amounts. The higher the muscovite content in the mixture, the higher the calcite and portlandite in their mineralogical composition. However, it is noticed that calcite and portlandite were the only cemented hydrates detected in CPB mixtures mineralogy and at very low rates. Muscovite rate was also very low relative to its real content in the mixture. These observations suggest that the presence of pure silica within the mixture affects the accuracy of XRD measurements, mainly in the identification and quantification of other mineral components, especially with interference from other silica-containing components such as muscovite.

Insights to the chemical composition of 7% CPB mixtures with different muscovite content was revealed using XRF analysis (Figure 8). Mixtures had a similar chemical composition with domination of three major oxides: SiO2, Al2O3 and CaO. The 7% CPB combine with either 12% or 18% muscovite show the highest K2O while 7% CPB/91 j indicated a high content of MgO.

Table 7. Mineralogy of 7%-CPB mixtures at 7 and 28 days.

Mineral	7-CPB-0%-7j	7-CPB-3%-7j	7-CPB-12%-7j	7-CPB-18%-7j	7-CPB-0%-28j	7-CPB-3%-28j	7-CPB-12%-28j	7-CPB-18%-28j
Quartz	98.8	98.2	94.4	92.3	95.5	96.6	92.9	94.6
Muscovite	n.d.	0.5	4	6.4	n.d.	1.7	2.6	4.9
Calcite	0.5	0.5	1.4	0.7	1.5	1.3	3.2	4.4
Portlandite	0.7	0.8	0.3	0.6	0.3	0.22	0.16	0.28

n.d. non detected.

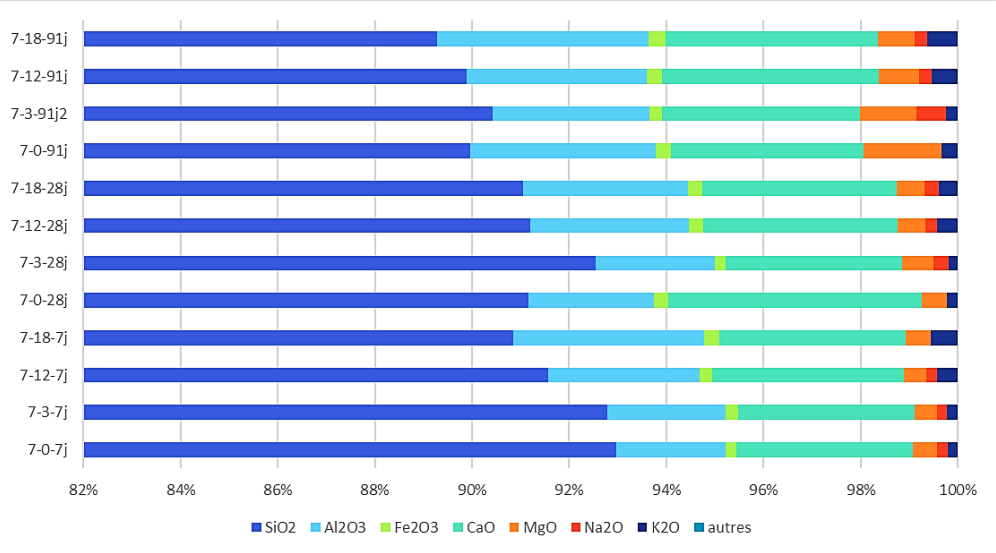

Figure 8. Chemical composition of 7% CPB mixtures at curing times of 7 and 28 days.

FTIR analysis

7% CPB/91 day mixtures were selected for FTIR analysis to identify and compare the chemical bands formed in the presence of muscovite. It was assumed that hydration process was well developed at 91 days, which explain the choice of mixtures at this curing time. Figure 9 assembles CPB spectra, showing a similarity among themselve with one important variation, notably the band with the visible peak reading located approx 3400–3600/cm. This band is associated with hydrogen bonding and the peak broadening is an indicator of interactions. The broadening can indicate that hydrogen bonding is present in a different state or in interactions with other molecules. According to literature, bands located at this range are associated to O-H stretching and can be interpreted as peaks for different potential constituents. For example, O-H bands located around 3422/cm indicates the presence of free water molecules; the same band can be located around 3610/cm and can be interpreted as a peak for free water (Šontevska, et al., 2008). O-H stretching bands located around 3415/cm, 3640/cm, and 3644/cm can be interpreted as peaks for portlandite (FARCAS et Touzé, 2001; Taylor, 1990) which agrees with XRD results. O-H bonding is exclusively detected within mixtures with muscovite content, while CPB-mixture of control (0%) does not have this band, indicating the presence of muscovite interactions within the mixtures.

Bands located around 1638/cm or 1477/cm can be also associated to O-H stretching bands and associated to portlandite (FARCAS et Touzé, 2001). However, these stretching bands have lower intensities compared to the peak broadening O-H band, which may indicate another state of hydrogen. C-O stretching bands at the same intensities stated for calcite are also detected around 875/cm and 710/cm (FARCAS & Touzé, 2001; Taylo, 1990). Portlandite and calcite were detected in all mixtures at the same range of absorbance, which likely because the presence of high pure Sil-Co-Sil causes interferences with other silica-containing components, negatively affecting both XRD and FTIR measurements. Stretching bands of Si-O are dominant in FTIR results. Silica-containing components were detected with FTIR, which confirms the problem of interference. Bands around 480/cm at the beginning of the spectra, and then at approx 1140/cm and 810/cm are associated with Si-O stretching within amorphous silica (FARCAS & Touzé, 2001).

A peak splitting between 900–1100/cm is also detected, associated with Si-O stretching (1022–1076/cm), Si-O-Si (990/cm), Al-O-H (908/cm), or potentially muscovite (Šontevska et al., 2008), as they do not appear in the 7% CPB/0% spectra, which is muscovite free. The shoulder peak with high intensity at approx 1310–1325/cm is present at the same absorbance in all the mixtures but remains unknown.

In general, FTIR analysis complies qualitatively with the XRD results and indicates the presence of potential interactions of O-H bonding. This can explain the sorption behavior of muscovite and the O-H bands are assumed to be associated with hydroxyls on the surface of muscovite layers.

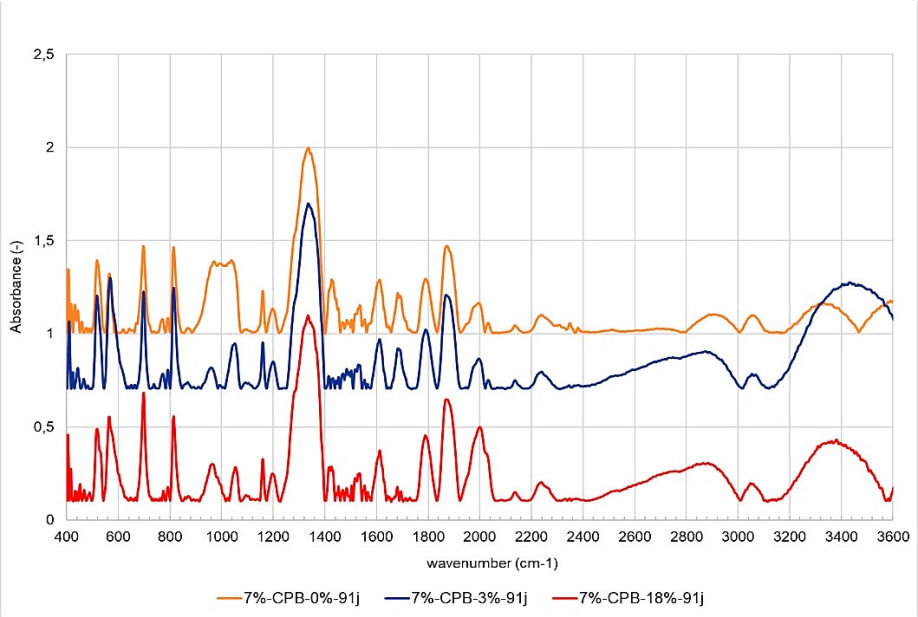

Figure 9. FTIR spectrums of 7% CPB/91 day mixtures.

Effect on water demand and water content

The amount of water added to each CPB mixture varied (Table 3). Results show that the higher muscovite amount in the mixture recipe, the more water is required to achieve the targeted slump (S_f). Figure 10 (a) illustrates the influence of muscovite content on water demand (WD). WD can be increased up to 19% to attend the targeted workability when muscovite content is increased up to 18% for mixtures made with 5% GU. The water demand rate seems to be less pronounced as binder content increases. For the same muscovite content (18%) plus 7% cement, water demand only increased up to 9%, which translated a positive contribution of cement content into compensating for increased water demand. The corresponding w/c ratios seem to increase slightly from 5.10–5.4 for 5% CPB-mixtures and from 7–8.35 for 7% CPB mixtures, which corresponds with the amount of water added to each mix. Table 8 presents mixture formulations and measured slump before (S_i) and after (S_f) mixing water addition. UCS measurements for mixtures at constant slump indicate a progressive decrease in UCS as muscovite content increases, this partially explained by the increased water in CPB mixture design. Figure 10 (b) presents the UCS-muscovite content plots with curing time. Water content (w%) was measured after UCS measurements. Figure 11 displays results of water content and curing time plots, where water content is normalized according to the CPB control mixture. Water content evolution followed the same trend for all studied mixtures: the higher the muscotive content, the higher water content, and the lower curing time, the higher water content, eg, a muscovite enrichment from 3% to 18% indicated an important increase in water content at 7 days (0.6 to 1.7) than at 91 days (0.6 to 0.8). This may be a consequence of hydration reactions that consumed water and/or by water retention through void spaces within muscovite or CPB particles.

Table 8. Water mass values and corresponding mini-cone slump measurements for studied CPB mixes.

Mixture			mini-S_i		mini-S_f	WD	
	g	-	*cm*	*g*	*cm*	*%*	-
5-CPB-0%	727.3	7	8.2	0	8.2	0.0	7
5-CPB-3%	727.3	7	7.0	33.9	8.8	4.7	6.68
5-CPB-12%	727.3	7	6.8	75.8	8.6	10.4	7.73
5-CPB-18%	727.3	7	6.1	140.74	8.7	19.4	8.35
7-CPB-0%	728.4	5.10	8.3	0	8.1	0.0	5.10
7-CPB-3%	728.4	5.10	7.6	40.5	8.6	5.6	5.38
7-CPB-12%	728.4	5.10	6.6	52.00	8.6	7.1	5.20
7-CPB-18%	728.4	5.10	6.4	71.5	8.6	9.8	5.39

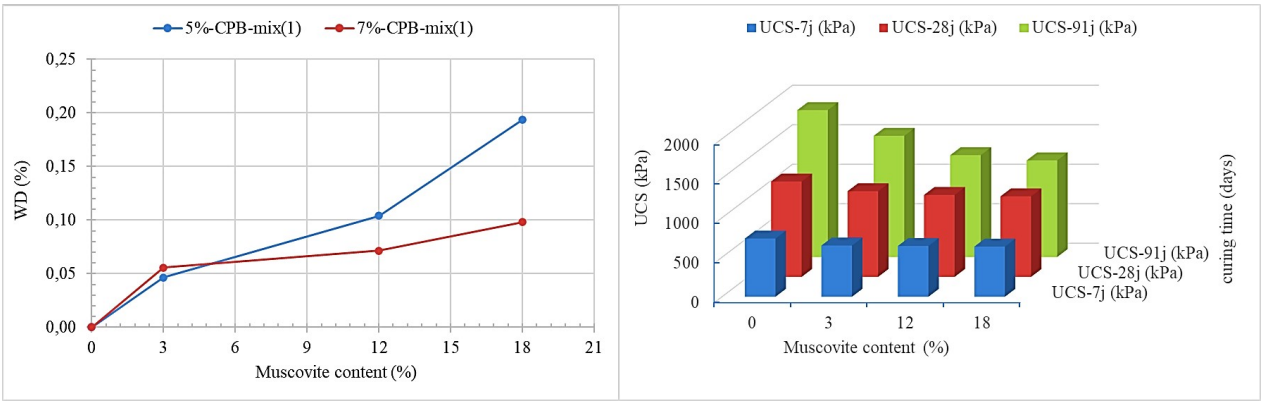

Figure 10. (a: left) water demand evolution of prepared CPB-mixtures influenced by muscovite content in the recipe; (b: right) UCS-muscovite content plots with curing time for CPB-mixtures at constant slump.

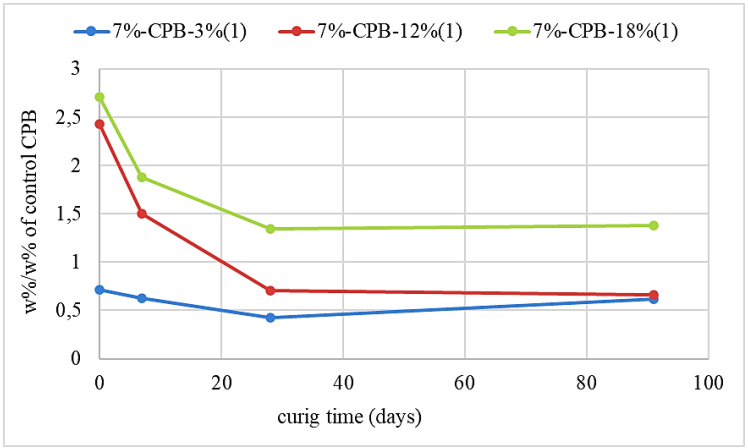

Figure 11. Evolution of water content with curing time for CPB-mixtures at constant slump.

Application to CPB mixes

To verify the trends reported experimentally in this study, multiple regression analysis with R software (R core Team, 2018) was applied and a correlation matrix was generated (Figure 13). Coefficients derived from the linear regression showed some significant correlation between WD, muscovite content, Bw, and UCS. At 7 days, UCS is mostly influenced by Bw, while at 91 days, both Bw and muscovite become equally influential on UCS (p-value of binder is greater than that of muscovite at both 7 and 28 days and becomes equal at 91 days). It seems that muscovite influence on UCS increases with curing time regardless of Bw. Moreover, muscovite is significantly influencing WD compared to Bw. Both linear regression models are significant; p-values of 0.004, 0.002 and 0.009 were obtained from testing for significance of the regression and coefficients of determination (R^2) of 0.88, 0.91 and 0.84, respectively, indicate high confidence of the analysis of variance (Figure 12).

```
Call:
lm(formula = UCS7j ~ Bw + Musco, data = Cor.UCS)

Residuals:
       1        2        3        4        5        6        7        8
 37.60185 -17.40337  -6.36902 -13.82946  20.63935 -49.96587   0.06848  29.25804

Coefficients:
            Estimate Std. Error t value Pr(>|t|)
(Intercept)  311.392     74.081   4.203  0.00846 **
Bw            57.981     11.966   4.846  0.00469 **
Musco         -6.165      1.672  -3.686  0.01420 *
---
Signif. codes:  0 ‘***’ 0.001 ‘**’ 0.01 ‘*’ 0.05 ‘.’ 0.1 ‘ ’ 1

Residual standard error: 33.84 on 5 degrees of freedom
Multiple R-squared:  0.8811,    Adjusted R-squared:  0.8336
F-statistic: 18.53 on 2 and 5 DF,  p-value: 0.00487

Call:
lm(formula = UCS91j ~ Bw + Musco, data = Cor.UCS)

Residuals:
      1       2       3       4       5       6       7       8
  47.52 -103.53  -32.10   88.11  151.37  -89.43  -82.17   20.23

Coefficients:
            Estimate Std. Error t value Pr(>|t|)
(Intercept)  315.245    239.467   1.316  0.24514
Bw           199.147     38.679   5.149  0.00362 **
Musco        -28.067      5.406  -5.192  0.00349 **
---
Signif. codes:  0 ‘***’ 0.001 ‘**’ 0.01 ‘*’ 0.05 ‘.’ 0.1 ‘ ’ 1

Residual standard error: 109.4 on 5 degrees of freedom
Multiple R-squared:  0.9145,    Adjusted R-squared:  0.8803
F-statistic: 26.73 on 2 and 5 DF,  p-value: 0.002139

Call:
lm(formula = WD ~ Bw + Musco, data = Cor.UCS)

Residuals:
       1        2        3        4        5        6        7        8
-0.027275 -0.001538 -0.009330  0.038143  0.003725  0.038462 -0.012330 -0.029857

Coefficients:
            Estimate Std. Error t value Pr(>|t|)
(Intercept)  0.104775   0.067995   1.541  0.18397
Bw          -0.015500   0.010983  -1.411  0.21724
Musco        0.007755   0.001535   5.052  0.00393 **
---
Signif. codes:  0 ‘***’ 0.001 ‘**’ 0.01 ‘*’ 0.05 ‘.’ 0.1 ‘ ’ 1

Residual standard error: 0.03106 on 5 degrees of freedom
Multiple R-squared:  0.8462,    Adjusted R-squared:  0.7847
F-statistic: 13.76 on 2 and 5 DF,  p-value: 0.009276
```

Figure 12. Linear regression models with predictors UCS 7 days (top), UCS 91 j (91 days; middle), and WD (bottom).

The correlation matrix (Figure 13) summarizes interactions between all combinations of predictor and response variables, and indicates:

- high positive correlation between muscovite and WD.
- high negative correlation with UCS 91 days and weak negative correlation with UCS 7 days and UCS 28 days, agreeing with p-value results in the model
- positive correlation between both Bw and UCS that decreases with UCS 91 days

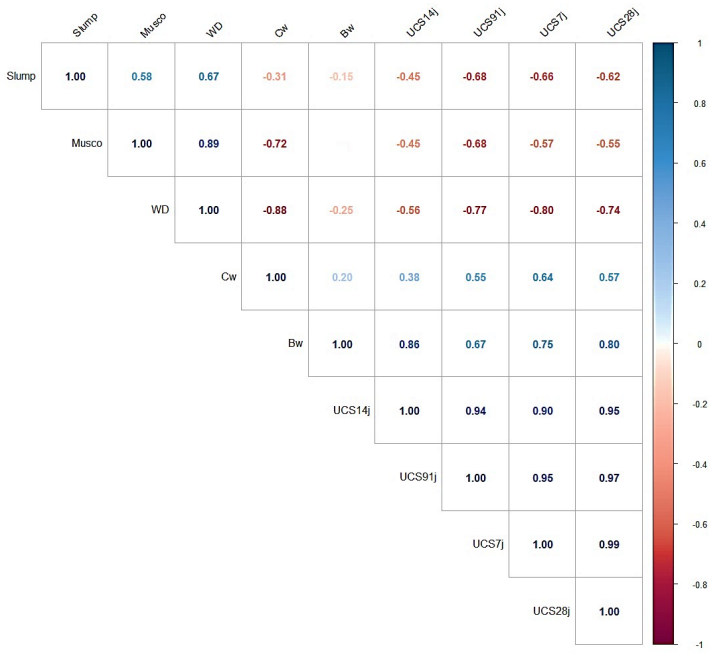

Figure 13. Correlation matrix between different variables and responses

Conclusion

This study focused on revealing the influence of muscovite content on CPB behavior using a systematic approach that address both quantitative and qualitative dimensions. First, CPB design recipes were prepared at fixed solid percentage C_w for both 5% and 7% Bw, where the only variable to change was muscovite content. This first set of experiments revealed that muscovite negatively influences CPB mechanical strength without the addition of water. The influence of muscovite was also explored through its impact on physical properties of the CPB, mainly specific surface area. The strength failure rate was slowed at high muscovite content and likely explained by increased void spacing. For the same recipes, some mineralogical and microstructural analyses were conducted, revealing the presence of significant O-H bonding related to absorbed water by muscovite, which likely impacted cement hydration processes and CPB hardening. A separate set of CPB recipes were prepared with varying amounts of water added to achieve a fixed slump to represent water content change within recipes. Results have shown that the higher the muscovite content, the higher the water demand required to achieve the targeted slump, and the lower the measured UCS. The phenomenon of strength decrease in CPB with rising mica content is therefore experimentally advocated.

References

ASTM. (2015). ASTM, C143/C143M-12 Standard Test Method for Slump of Hydraulic- Cement Concrete. In *Annu. B. ASTM Stand* (pp. pp. 1–4). https://doi.org/https://doi.org/10.1520/ C0143_C0143M-12

ASTM. (2021). ASTM C39/C39m-21 standard test method for compressive strength of cylindrical concrete specimens. In *Annu. Book ASTM Stand.* (pp. 1–8). https://doi.org/https:// doi.org/10.1520/C0039_C0039M-21, 04.02

Belem, T., & Benzaazoua, M. (2007). Design and Application of Underground Mine Paste Backfill Technology. *Geotechnical and Geological Engineering*, *26*(2), 147-174. https://doi.org/10.1007/s10706-007-9154-3

Belem, T., & Benzaazoua, M. (2008). Design and application of underground mine paste backfill technology. *Geotechnical and Geological Engineering*, *26*, 147-174.

Belem, T., Benzaazoua, M., & Bussière, B. (2003). Utilisation du remblai en pâte comme support de terrain. Partie I: De sa fabrication à sa mise en place sous terre. Symp. int. Apres-mines, GISOS, Gisos ed., Nancy, France,

Benzaazoua, M., Belem, T., & Bussiere, B. (2002). Chemical factors that influence the performance of mine sulphidic paste backfill. *Cement and Concrete Research*, *32*(7), 1133-1144.

Benzaazoua, M., Fall, M., & Belem, T. (2004). A contribution to understanding the hardening process of cemented pastefill. *Minerals Engineering*, *17*(2), 141-152.

Dewar, J. (1963). *Effect of mica in the fine aggregate on the water requirement and strength of concrete. cement and concrete association*.

Ercikdi, B., Cihangir, F., Kesimal, A., Deveci, H., & Alp, İ. (2009). Utilization of industrial waste products as pozzolanic material in cemented paste backfill of high sulphide mill tailings. *Journal of Hazardous Materials*, *168*(2), 848-856. https://doi.org/https://doi.org/10.1016/j.jhazmat.2009.02.100

Farcas, F., & Touze, P. (2001). La spectrométrie infrarouge à transformée de Fourier (IRTF). *Une méthode intéressante pour la caractérisation des ciments (in French) Bull. Lab. Ponts Chaussées*, *230*, 77-88.

Ferraris, C. F., & de Larrard, F. (1998). Modified slump test to measure rheological parameters of fresh concrete. *Cement, Concrete, and Aggregates*, *20*(2), 241-247.

Ko, T. N. N. (2019). Experimental Research on the Behavior of Concrete Using Mica as Partial Replacement of Fine Aggregates.

Lagerblad, B., Westerholm, B. L. M., Gram, M. W. H.-E., Westerholm, M., Gram, H.-E., Attenius, E., & Fjällberg, L. (2005). Krossad berg som ballast till betong. *Crushed rock as concrete aggregate). Report from the Swedish national project" MinBaS (Compilation of 6 project reports), CBI, Stockholm. In Swedish*.

Lagerblad, B., Gram, H.-E., & Westerholm, M. (2014). Evaluation of the quality of fine materials and filler from crushed rocks in concrete production. *Construction and Building Materials*, *67*, 121-126. https://doi.org/10.1016/j.conbuildmat.2013.10.029

Leemann, A., Lothenbach, B., Münch, B., Campbell, T., & Dunlop, P. (2023). The "mica crisis" in Donegal, Ireland–A case of internal sulfate attack? *Cement and Concrete Research*, *168*, 107149.

Loorents, K.-J., Johansson, E., & Arvidsson, H. (2007). Free mica grains in crushed rock aggregates. *Bulletin of Engineering Geology and the Environment*, *66*, 441-447.

Mantellato, S., Palacios, M., & Flatt, R. J. (2015). Reliable specific surface area measurements on anhydrous cements. *Cement and Concrete Research*, *67*, 286-291.

Maregesi, G. R., & Salaam-Tanzania, D. E. SOME ENGINEERING PROPERTIES OF UDZUNGWA SCARP SOIL.

Mehdipour, I., & Khayat, K. H. (2017). Effect of particle-size distribution and specific surface area of different binder systems on packing density and flow characteristics of cement paste. *Cement and concrete composites*, *78*, 120-131.

Mshali, M., & Visser, A. (2014). Influence of mica on compactability and moisture content of cement-treated weathered granite gravel.

Mshali, M., & Visser, A. T. (2012). Influence of mica on unconfined compressive strength of a cement-treated weathered granite gravel. *Journal of the South African Institution of Civil Engineering= Joernaal van die Suid-Afrikaanse Instituut van Siviele Ingenieurswese*, *54*(2), 71-77.

Muller, O. (1971). Some aspects of the effect of micaceous sand on concrete. *Civil Engineering= Siviele Ingenieurswese*, *1971*(9), 313-315.

Ouattara, D. (2017). *Étude expérimentale des propriétés rhéologiques et mécaniques des remblais miniers en pâte cimentés incorporant des superplastifiants*. Thèse de doctorat à l'Université du Québec en Abitibi Téminscamingue (UQAT), Québec, Canada.

Ouffa, N. (2019). *Solubilité de différents minéraux aluminosilicatés en vue de leur contribution à la géopolymérisation dans les remblais miniers en pâte*. Ecole Polytechnique, Montreal (Canada).

Patil, M. V., & Patil, Y. D. (2021). Effect of copper slag and granite dust as sand replacement on the properties of concrete. *Materials Today: Proceedings*, *43*, 1666-1677.

Pillet, M. (2001). *Les plans d'expériences par la méthode Taguchi*. Maurice Pillet.

Roussel, N., Stéfani, C., & Leroy, R. (2005). From mini-cone test to Abrams cone test: measurement of cement-based materials yield stress using slump tests. *Cement and Concrete Research*, *35*(5), 817-822.

Sadat Alhosseini, R. (2009). *Development of an Artificial Neural Network (ANN) Model for Estimating Cemented Paste Backfill Performance* Université du Québec en Abitibi-Témiscamingue].

Schmitt, J. W. (1990). Effects of mica, aggregate coatings, and water-soluble impurities on concrete. *Concrete International*, *12*(12), 54-58.

Seifi, S., Levacher, D., Razakamanantsoa, A., & Sebaibi, N. (2023). Microstructure of Dry Mortars without Cement: Specific Surface Area, Pore Size and Volume Distribution Analysis. *Applied Sciences*, *13*(9), 5616.

Snellings, R., Machner, A., Bolte, G., Kamyab, H., Durdzinski, P., Teck, P., Zajac, M., Muller, A., de Weerdt, K., & Haha, M. B. (2022). Hydration kinetics of ternary slag-limestone cements: Impact of water to binder ratio and curing temperature. *Cement and Concrete Research*, *151*, 106647.

Šontevska, V., Jovanovski, G., Makreski, P., Raškovska, A., & Šoptrajanov, B. (2008). Minerals from Macedonia. XXI. Vibrational spectroscopy as identificational tool for some phyllosilicate minerals. *Acta Chimica Slovenica, 55 (4), 757–766 (2008)*.

Tan, Z., Bernal, S. A., & Provis, J. L. (2017). Reproducible mini-slump test procedure for measuring the yield stress of cementitious pastes. *Materials and Structures*, *50*, 1-12.

Tarefder, R., Faisal, H., & Sobien, H. (2014). Nanomechanical characterization effect of mica and aging on asphalt binder. *Journal of Materials in Civil Engineering*, *26*(9), 04014063.

Tariq, A., & Yanful, E. K. (2013). A review of binders used in cemented paste tailings for underground and surface disposal practices. *Journal of environmental management*, *131*, 138-149.

Taylor, W. (1990). Application of infrared spectroscopy to studies of silicate glass structure: Examples from the melilite glasses and the systems Na 2 O-SiO 2 and Na 2 O-Al 2 O 3-SiO 2. *Proceedings of the Indian Academy of Sciences-Earth and Planetary Sciences*, *99*, 99-117.

Tugrul, A., Hasdemir, S., & Yılmaz, M. (2015). The effect of feldspar, mica and clay minerals on compressive strength of mortar. Engineering Geology for Society and Territory-Volume 5: Urban Geology, Sustainable Planning and Landscape Exploitation,

Xing, J. Q., Zhan, S. L., & Li, X. Y. (2014). Effect of mica content in stone powder of manufactured sand on performance of cement mortar. *Advanced Materials Research*, *1044*, 624-628.